Article

Journal of
Nanoscience and Nanotechnology
Vol. 18, 668–675, 2018
www.aspbs.com/jnn

Enhanced Swelling, Mechanical and Thermal Properties of Cellulose Nanofibrils (CNF)/Poly(vinyl alcohol) (PVA) Hydrogels with Controlled Porous Structure

Zhao-Yang Xu* and Jian-Yu Li

College of Materials Science and Engineering, Nanjing Forestry University, Nanjing, Jiangsu 210037, China

In this work, novel porous cellulose nanofibrils (CNF)/poly(vinyl alcohol) (PVA) hydrogels were prepared using the hybrid solvent of dimethyl sulfoxide (DMSO)/water, followed by freezing/thawing process. Structure, swelling, mechanical and thermal properties of CNF/PVA were explored. The results revealed that porous hydrogels were formed by using the hybrid solvent of DMSO/water, and the pore sizes of hydrogels were controlled by the concentration of CNF. The porous structure of the composite hydrogels can strongly enhance the swelling properties as expected. Compared with pure PVA hydrogels, a 150% improvement in compressive strength were achieved by the hybrid solvent. And the increment of compressive strength depended on the concentration of the CNF. Moreover, the addition of CNF improved the thermal stability of the PVA hydrogels significantly. The low cost, nontoxic and high-performance nanoreinforced hydrogels may have a promising application in tissue engineering fields.

Keywords: Biomaterials, Porous Materials, Thermal Properties, Mechanical Properties.

1. INTRODUCTION

Hydrogels are viscoelastic and crosslinked networks polymers that are capable of adsorbing considerable amount of water while maintaining network integrity.[1–4] Considering their properties of high water up-take, moisture retention, and good biocompatibility, hydrogels are particularly attractive for biomedical and pharmaceutical applications such as wound dressing, drug delivery systems and tissue engineering.[5–7]

Much attention has been directed in recent years to porous hydrogels, because introduction of pores into hydrogels could be used to improve biological response and lead to improved outcomes in biomedical applications.[8, 9] The introduction of porous structure not only provides more space for cell migration and tissue invasion but also increases the surface area to volume ratio which can enable more efficient mass transport to the developing tissue.[10, 11] Therefore, it is crucial to control the various pore features such as pore size, pore distribution, porosity and interconnectivity within hydrogels.

Several techniques have been employed to generate porous to hydrogels, such as porogen extraction, chemically inducing phase separation, foaming and solvent casting/particulate leaching.[10, 12] In a method studied by Chiu et al.,[11] porous poly(ethylene glycol)-poly(*L*-lactic acid) hydrogels were generated by solvent casting/particulate leaching and photopolymerization. The result showed that the initial pore size depended on particulate size but not polymer concentration, while degradation time was dependent on polymer concentration. Cheng et al.[13] produced porous poly(*N*-isopropylacrylamide) (PNIPAAm) hydrogels through phase separation of PNIPAAm in aqueous sodium chloride solutions with different concentrations. The PNIPA gels thus prepared had remarkably larger swelling ratios below their lower critical solution temperature (LCST) in comparison with conventional PNIPA hydrogels, and exhibited much faster response rates as the temperature was raised above their LCST. Large amounts of researches have shown how to fabricate the porous hydrogels by chemical method, however, control of the pore distribution (which is often random) and pore size or type of monomer are limited in these methods.[14] Besides, the chemical agents introduced in preparation of

*Author to whom correspondence should be addressed.

 1533-4880/2018/18/668/008 doi:10.1166/jnn.2018.14185

hydrogels are often toxic, inevitably affect the biocompatibility of hydrogels. Therefore, methods for fabricating porous hydrogels still remain challenges.

Poly(vinyl alcohol) (PVA) hydrogels have been studied extensively and considered as one of the most suitable hydrogels for tissue engineering, drug delivery and biomedical applications due to its biocompatibility and nontoxicity. In addition, it also presents many excellent properties such as chemical property stability, the availability and low cost of the molding.[15–20] Recently, some researches have been performed using technique of the mixed solutions to expand the application of PVA hydrogel in the biomedical field. Jiang et al.[21] investigated a Poly(vinyl alcohol) (PVA) hydrogel as tissue equivalent material which was used in accurate surgical insertion research. The PVA hydrogel was prepared by means of physical and chemical crosslink, in which mixed solutions of dimethyl sulfoxide/de-ionized water/NaCl (DMSO/H_2O/NaCl) were prepared as the solvent. The results demonstrated that this tissue equivalent material could be used in the *ex vivo* insertion accuracy test for robot-assisted percutaneous intervention and surgical training in minimally invasive surgery. In a different work, Jiang et al.[22] developed a PVA hydrogel by chemical cross-linking which contained DMSO and porcine small intestinal submucosa (SIS) powders. The results of mechanical and biocompatible testing showed that mechanical properties, blood and cell compatibility of the hydrogels were changed when the DMSO was added in PVA-SIS system. So far, however, a few research has applied the hybrid solvent of DMSO/water to fabricate porous hydrogels.

Our goal was to prepare porous hydroges with improved performance through a reliable and facile way. In this study, porous CNF/PVA hydrogels with controlled porous structure were synthesized using the hybrid solvent of DMSO/water, followed by freezing/thawing process. To the best of our knowledge, this is the first report on the physical structure and properties of porous CNF/PVA hydrogels based on the hybrid solvent of DMSO/water and freezing/thawing process. The structure and properties of hydrogels were characterized by scanning electron microscopy (SEM), Fourier transform infrared spectroscopy (FTIR), X-ray diffraction (XRD), Compression tests, Swelling ratio tests, and Thermal stability measurements. We hope to provide valuable relationship information of the porous hydrogels between structure and properties for applications of these nanocomposite hydrogels.

2. MATERIALS AND METHODS

2.1. Materials

Bamboo sawdust purchased from Zhejiang (Lishui, China) was sieved through a 60 mesh prior to further treatments. Poly(vinyl alcohol) with an average degree of polymerization of 1750 ± 50, benzene, ethanol, dimethyl sulfoxide, sodium chlorite, glacial acetic acid, potassium hydroxide and hydrogen chloride were all obtained from Nanjing Chemical Reagent Co., Ltd. All the chemicals were used without any further treatment.

2.2. Methods

2.2.1. Preparation of CNF

The CNF was prepared from bamboo sawdust. It was chemically purified according to literature method[23] and adapted with appropriate modifications according to our previous work.[24] Bamboo sawdust (10 g) was extracted by benzene ethanol at 90 °C for 6 h. 400 mL distilled water was added into sealed flasks of treated bamboo sawdust, then adding 5 g sodium hypochlorite and 2 mL acetic acid every hour, stirring for 5 h in water bath at 75 °C. The suspensions were cooled to room temperature and then washed with distilled water to neutral. After that, the obtained materials were added into 2.0 wt% potassium hydroxide with stirring at 90 °C for 2 h, and then washed to neutral with distilled water. Changing the stirring time to 1 h when the same amount of sodium hypochlorite and acetic acid were added into sealed flasks with 400 mL distilled water. Then the stirring step was repeated when the concentration of KOH solution changed to 5.0 wt%. Pure cellulose was obtained when the final suspensions were washed to neutral. Hydrogen chloride solution of 1.5 wt% was used to degrade cellulose. Finally, CNF suspension was prepared by beating 1.0 wt% cellulose suspension within a grinder (MKCA6-2, Masuko Sangyo Co., Ltd., Japan) at 1500 rpm[25] and stored for further utilization.

2.2.2. Preparation of CNF/PVA Hydrogels

The preparation process of the crosslinked CNF/PVA hydrogels is shown schematically in Figure 1. Different concentrations of CNF suspension were obtained by adding a desired amount of water. 7.5 g PVA was dissolved in 100 g mixture of CNF suspension (the CNF solid content varied from 0, 2.5, 5.0, 7.5 and 10.0% of the PVA mass) and DMSO with stirring at 95 °C for 3 h. The weight ratio between the water of CNF suspension and DMSO was 1:4 for all formulations. Then the mixture was set aside for 30 min at 60 °C to remove the air bubbles and became homogeneous and viscous gradually. The mixture was then poured into 24 orifices and frozen at −20 °C for 12 h and followed by thawing at 25 °C for 4 h, completing one freezing/thawing cycle. This freezing/thawing cycle was repeated up to five times. Then the hydrogels obtained were submerged in distilled water to extract DMSO. The CNF/PVA hydrogels were coded as 0%CNF, 2.5%CNF, 5.0%CNF, 7.5%CNF, 10.0%CNF, corresponding to a CNF content of 0, 2.5, 5.0, 7.5 and 10.0 wt%, respectively. In order to compare with PVA hydrogels obtained from water/DMSO, the PVA hydrogel formed with water alone was prepared.

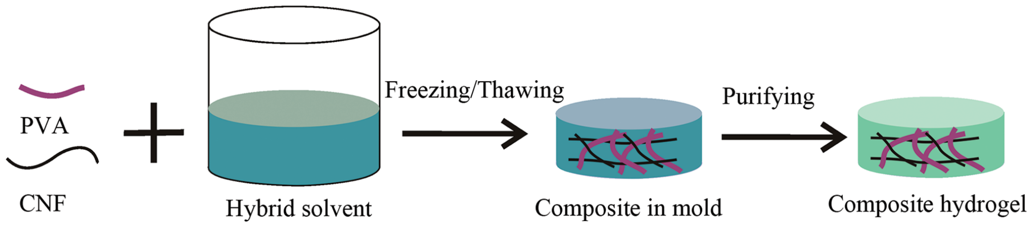

Figure 1. Scheme of the preparation of composite CNF/PVA hydrogels.

3. CHARACTERIZATION

The scanning electron microscopy was performed to investigate the morphology of the samples with a Hitachi S-4800. The SEM observation of freeze-dried CNF and hydrogels samples were frozen in liquid nitrogen and snapped immediately before being fractured and coated with gold for 60 s. Pore analysis was performed using the public domain ImageJ software[26] developed at the US National Institutes of Health (NIH) (available at http://rsb.info.nih. gov/ij/). ImageJ software was used to measure the sample pores selected on SEM images for each type of sample. The SEM images were taken at random locations across cross-sections of the hydrogels, and the values of pore size generated from three images were used to calculate the average pore size for each sample. The CNF, PVA crystalline structure and interaction in the hydrogels were analyzed by FTIR (Nicolet iS10, Thermo Electron Corp. USA) spectrophotometer with an attenuated total reflectance (ATR) device in the region of 500–4000 cm^{-1} with a resolution of 4 cm^{-1}. All the hydrogels samples have equal thickness and were freeze-dried before analyzed. The X-ray diffraction patterns of the dried sheets were recorded on X-ray diffraction instrument (Ultima IV, Rigaku, Japan) in terms of a Cu K a radiation at 40 kV and 30 mA. All samples were analyzed in the angular range of 5°–50° (2θ) at a scanning rate of 5°/min. Swelling ratio measurement was to study the effects of CNF content on the hydrogels properties at equilibrium in water. The hydrogels samples were immersed in distilled water at 25 °C for 24 h to reach the swelling equilibrium. The weights of the hydrogels were recorded after the hydrogels surfaces were wiped to remove excess water with filter papers. The equilibrium swelling ratio (SR%) was calculated using the equation:

$$SR(\%) = 100 * (W_s - W_d)/W_d \quad (1)$$

Where W_s is the swollen hydrogels weight at 25 °C, W_d is the hydrogels weight at dry state. Compression tests were performed by using the universal mechanical (SANS Test machine Co. Ltd., Shenzhen, China) fitted with a 1 kN load at a speed of 5 mm/min until the strain reaches 60% at room temperature. The hydrogel samples applied in the mechanical testing were in equilibrated swelling state with a cylindrical shape of 12 mm in diameter and 12 mm in height. Five specimens were tested for each sample under the same conditions. Thermal stability measurements were carried out using a thermogravimetric analyzer (TGA, 209F3, NETSCH, Germany). The dry samples weighing between 3 and 10 mg were packed in aluminum pans and tested from 30 °C to 600 °C at a heating rate of 10 °C/min under nitrogen atmosphere.

4. RESULTS AND DISCUSSION

4.1. Cross-Linking Interactions in Composite Hydrogels

The formation mechanism of PVA hydrogel is widely believed that the aqueous PVA phase crystallized during freezing/thawing cycles at low temperature, and the subsequent alignment of the polymer chains in the liquid part of the PVA, which then hydrogen bond to each other.[8, 10] Intrachain physical cross-links are formed between the PVA hydroxyl groups, and owing to numerous hydroxyl groups of CNF, interchain cross-links are formed between the hydroxyl groups of CNF and PVA. During the formation of the cross-linked network between CNF and PVA matrix, these hydrogen bonds act as physical cross-linking points.

Figure 2 showed the FTIR spectra of the CNF, PVA and CNF/PVA hydrogels. An important absorption peak at 1143 cm^{-1} was observed in all hydrogels, which is related to the C–C stretching vibration of PVA and associated with the crystallinity of PVA.[27] The stretching vibration at 1090 cm^{-1} is the characteristic C–O absorption band of PVA. The absorptions in the spectra of CNF at 1053 and 896 cm^{-1} are C–O stretching and anomeric carbon of β-D-glucopyranosyl in cellulose, which is coinciding with the reported data.[15] For pure PVA hydrogels, the stretching vibration of –OH groups at 3278 cm^{-1} exhibited a strong absorption peak centered, arising from the hydrogen bonding interactions in PVA. For 0%CNF sample, the –OH groups stretching vibration exhibited a strong absorption peak centered at 3274 cm^{-1}. This absorption peak gradually shifted to lower wavenumber at 3258 cm^{-1} with the increment of CNF contents in the PVA matrix, confirming that hydrogen existed between the PVA and CNF.

To further identify the intermolecular interactions in CNF/PVA hydrogels, XRD analysis was performed. As shown in Figure 3, all CNF/PVA hydrogels samples exhibited a crystalline structure with a peak angle around $2\theta = 19.5°$, which was assigned to crystalline segment of PVA.[28]

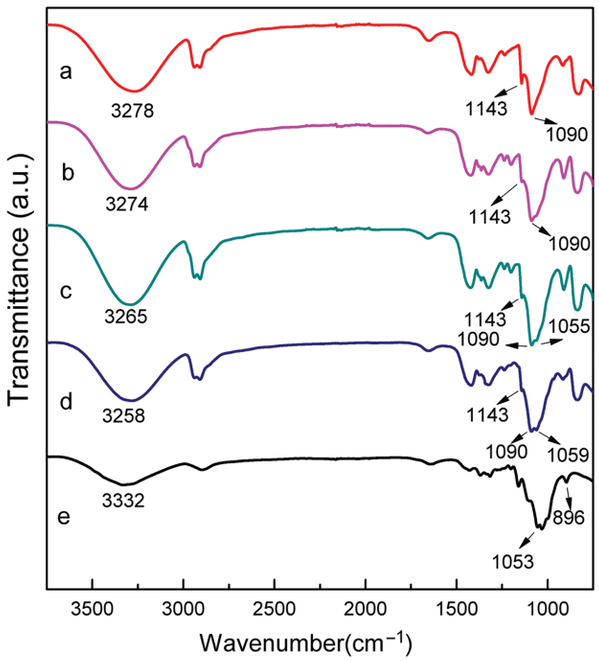

Figure 2. FTIR spectra of the CNF, PVA and CNF/PVA hydrogels: (a) 0, (b) 2.5%CNF, (c) 7.5%CNF, (d) 10.0%CNF, (e) CNF.

The diffraction peaks of the angles at about $2\theta = 22.5°$ and 16° (Figs. 2(b, d)) were related to the typical reflection (002), (101) planes of cellulose I,[15] respectively. With the increment of CNF content in PVA hydrogels, the intensity of the peaks around $2\theta = 19.5°$ decreased. This evidence revealed that intermolecular interactions between CNF and PVA molecule formed in the nanocomposites. It was reported by Liu et al.[15] that there was a linear relationship between the crystallinity and the content of CNF in the composites, with the increment of the content of CNF, the crystallinity of the PVA/CNF composites increased accordingly. In view of these results, the hydrogen bonding interactions existed and caused by CNF and PVA in the composite hydrogels.

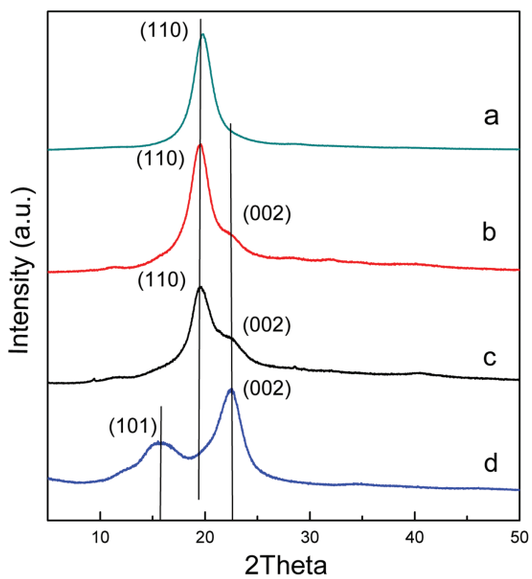

Figure 3. X-ray diffraction patterns of samples: (a) 0, (b) 2.5%CNF, (c) 10.0%CNF, (d) CNF.

4.2. Morphologies and Structure of CNF and Composite Hydrogels

Figure 4(a) showed the photograph of CNF suspension and Figure 4(b) showed the SEM image of freeze-dried CNF sample. It was clear that the CNF displayed a network structure with a diameter in the range from 10 to 30 nm. The SEM images of composite hydrogels cross-section were shown in Figure 5. The pore size distribution and average pore size of hydrogels samples determined from ImageJ software were summarized in Table I. Figure 5(a) revealed a rough surface morphology of the pure PVA hydrogels with a few irregular and heterogeneous pores structure which was not well interconnected. All of the composite hydrogels exhibited a homogeneous porous structure with different pore sizes, as shown in Figures 5(b–f). Compared with the hydrogels prepared from water alone, microscopic structure of composites hydrogels obtained from hybrid solvent changed significantly. Such porous structure indicated that adding organic solvents into the PVA solution could develop well-distributed changes on the microscopic structure. This could be explained as DMSO is a kind of protophobic solvent, the molecular chain of PVA was greatly extended and each PVA molecule was surrounded by almost the same number of water molecules when the PVA dissolved in DMSO/water mixture.[29, 30] The formation of DMSO/water complexes in the medium affected the rate and mechanism of PVA gelation, the simultaneous presence of liquid DMSO/water complexes perhaps disrupted the normal growth of ice crystals, leading to different structure and properties of the hydrogels. So, in the process of forming a gel it can form a uniform cross-linked network structure. A recent study from Hou et al.[31] had also proved that O atoms in DMSO preferentially

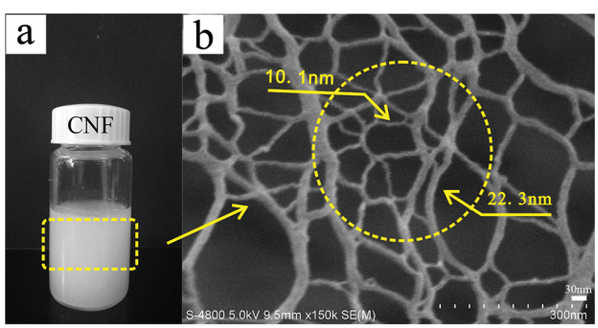

Figure 4. Photograph of CNF suspension (a) and SEM image of CNF after freeze-dried (b).

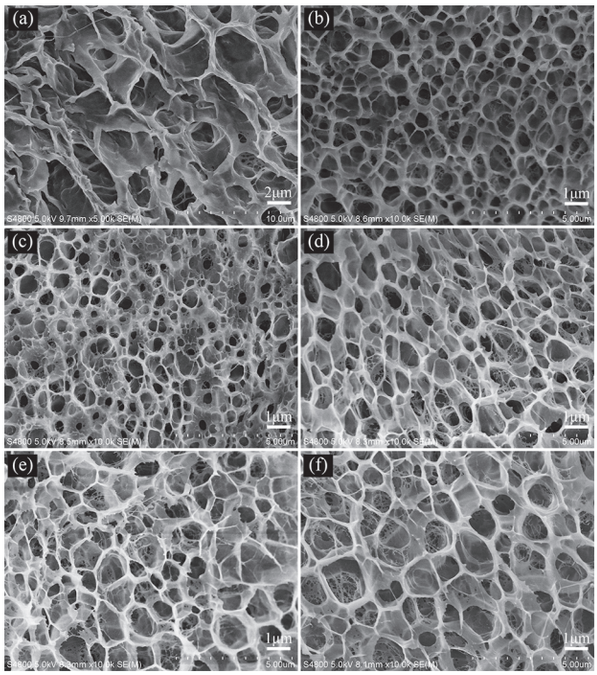

Figure 5. SEM images of cross-section of the (a) PVA hydrogel formed with pure water and H_2O/DMSO boosted CNF/PVA hydrogels with different contents of CNF: (b) 0, (c) 2.5%CNF, (d) 5.0%CNF, (e) 7.5%CNF, and (f) 10.0%CNF.

combined with the active H atoms in H_2O, showing a tendency to form 1DMSO/2H_2O network structure. Thus, a three dimensional crosslinking structure of PVA hydrogel appeared.

The introduction of enhanced pores can provide more space and increase surface area-to-volume ratio of hydrogels for tissue invasion, facilitate nutrient transport, and cell growth and local angiogenesis, as reported by Kamoun et al.[32] In another study, Huang et al.[33] reported that pore size is important for regulating cell behavior, such as amoeboid-like changes of mammalian and cells neovascularization. Thus, it has a significant meaning to synthesize and control the porous structure of hydrogels. For PVA hydrogels prepared by water alone in this work, the pore size was distributed within the range of 1.37∼3.61 μm with average pore size of 1.93 μm. The pore size distribution was wide range, and as mentioned above, the porous structure was not well interconnected. These would limit the application of hydrogels in the biological field. On the other hand, hydrogels samples prepared using water/DMSO, the pore size was in the submicrometer range. The general morphological trend observed was an apparent shift of the pore size distribution to larger pores (except for the slight decrease of 2.5% CNF) as the CNF loading increased from 0% to 10.0% after the freezing/thawing cycles (average pore size from 0.69 μm to 1.09 μm).

The pore sizes were thought to reflect the dimensions of the ice regions formed during the freezing/thawing cycles as suggested by Abitbol et al.,[34] which in turn will be influenced by the PVA and CNF concentrations. The larger pores observed in the hydrogels may thus be due to the decrease in free PVA volume fraction in the presence of higher CNF concentrations. For instance, Yokoyama et al.[35] reported an increment in pore size of hydrogels with decreasing concentration of PVA. Therefore, it is reasonable that the CNF played a significant role in the controlling of the pores structures and dimensional stability of the PVA hydrogels.

4.3. Swelling Ratio of Composites Hydrogels

The equilibrium swelling ratio of composite hydrogels can also reflect the change in the pore size. The swelling ratio of composite CNF/PVA hydrogels in distilled water was presented in Figure 6. Compared to the PVA hydrogels prepared by water alone, the swelling ratio of PVA hydrogels prepared by hybrid solvent increased from 568% to 770%. The swelling ratio was greatly improved due to the formation of porous structure. It was not hard to imagine that more porous structures make water molecules transfer easier between the hydrogels matrix and the external aqueous phase; Meanwhile, the porous structure provided more storage space for water molecules. As the CNF imparted to the hydrogels, the equilibrium swelling ratio of hydrogels increased significantly (from 795% to 935%) with an increment of CNF content. This was attributed to enlarged pore size of hydrogels as well as the hydrophilic nature of CNF. Previous studies have found that water content in PVA hydrogels is not only to provide a local moist environment (which is a key factor for wound healing rate), but also to adjust the permeation of nutrients, drug, gases, or protein into the cells or targeted absorption site.[33] The absorption capacities of the CNF/PVA hydrogels were much higher than that of the PVA hydrogels prepared by water alone, which further confirmed the importance of composite hydrogels with highly porous structures and controlled pore size. It is quite important in their further applications to maintain a high swelling ratio for these biocompatibility and bioactivity materials.

Table I. The pore size distribution and average pore size of hydrogels samples.

		Water/DMSO (μm)				
	Pure water (μm)	0%CNF	2.5%CNF	5.0%CNF	7.5%CNF	10.0%CNF
Distribution range	1.37∼3.61	0.58∼0.83	0.42∼0.89	0.54∼1.02	0.72∼1.25	0.75∼1.59
Average size	1.93	0.69	0.65	0.73	0.93	1.09

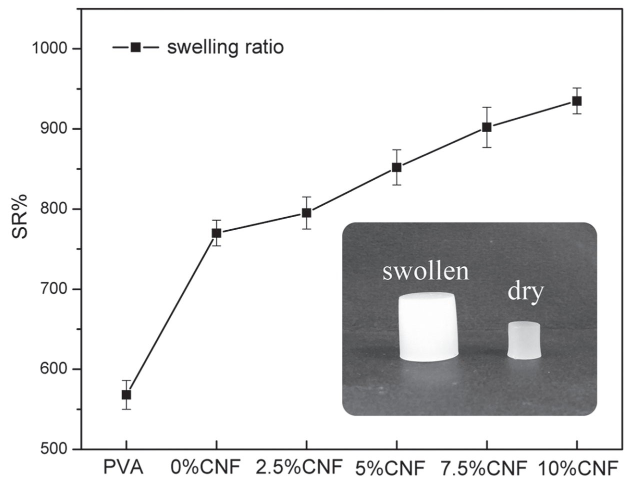

Figure 6. Swelling ratio of composite hydrogels, and photograph of composite hydrogels at the swollen and dry state.

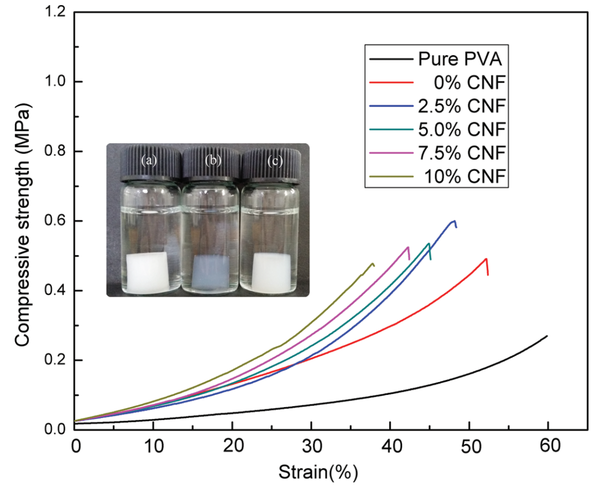

Figure 7. Typical stress–strain curves and photographs of the hydrogels with different CNF contents: (a) Pure PVA hydrogel, (b) 0%CNF, (c) 10%CNF.

However, there are many factors that affect the swelling ratio, such as pore sizes, pore geometry, pore surface area, and degrees of interconnection within porous structures.[8,36] It is worth noting that the reinforced materials also play an important role in swelling ratio. A recent research by Ren et al.[37] have demonstrated that strong internetwork interaction caused the decrease in intermolecular space when excessive regenerated cellulose molecule chains occupied the original amorphous region of PVA hydrogels, which prevented the water from being absorbed. Thus, it is reasonable to assume that the swelling ratio of composite hydrogels will decrease when the CNF reaches a certain amount. Studies are currently underway to correlate the swelling and transmission properties of porous hydrogels with porosity and inter connectivity.

4.4. Mechanical Properties of Composite Hydrogels

Compressive test was performed to evaluate the effect of the introduction of hybrid solvent and CNF into PVA hydrogels on mechanical property. Also the photographs of the hydrogels with different CNF contents were shown in Figure 7. Clearly, all of the composite hydrogels exhibited good processability and appearance. Conclusion can be drawn from Figure 7 that the stress–strain behavior of all hydrogels presented an exponential relationship. With the increment of force loading, the orientation and relative position of PVA chains in the PVA hydrogels were thought to change and the interstitial water began to be squeezed out,[38] so the stress increased with the increasing strain. As further increment of the strain, chain orientation tended to be uniform; The interspace for chain moving was compressed and limited, which caused stress to rise increasingly quicker at a higher strain. As shown in Figure 7, the pure PVA hydrogels exhibited the lowest compressive strength (0.27 MPa, strain at 60%). For composite hydrogels, the three-dimensional network structure was rigid[38] and the CNF cannot move like PVA chains, which caused much more resistant of hydrogels to deformation at a given load. Obviously, the compressive strength of 0%CNF/PVA hydrogels was 2.5 times higher than that of the pure PVA hydrogels (strain at break of 53%), as a result of the reinforcement caused by the porous networks. With the addition of CNF, the compressive strength of the composites was improved, indicating the reinforcement role of CNF on composite hydrogels. In Figure 7, 2.5%CNF/PVA hydrogels had the best compressive fracture strength of 0.6 MPa (strain at break of 47%), which was attributed to the small porous structure (Fig. 4 and Table I) and the reinforcement of CNF.

The pore size, pore morphology and interconnectivity are interrelated and influence the permeability of fluid through hydrogels as well as its mechanical properties, as suggested by Spiller et al.[8] Indeed, a decrease in pore size or increament in cross-linking density generally leads to harder and stronger hydrogels, due to the smaller pore size and more cross-linking points would cause the better stress dispersion.[33,37] During the freezing/thawing process, the strong hydrogen bonding formed between CNF and PVA actually acts as physical cross-linking points. With the CNF content increasing, the increased hydrogen bondings and the density of network lead to a compact and stable porous structure. Thus, during the compression process, the porous structure with strong interaction possessed high compressive strength, and CNF with high strength and modulus was contributed to enhance the compressive strength. In addition, with the increment in CNF content, cellulose network tended to play a skeleton structure role, acting as the major part to support the entire porous structure of the composite hydrogels, even after the PVA matrix collapsed. This may explain the result of compressive fracture strain decreased with increment of pore size. The mechanism was presented in Figure 8.

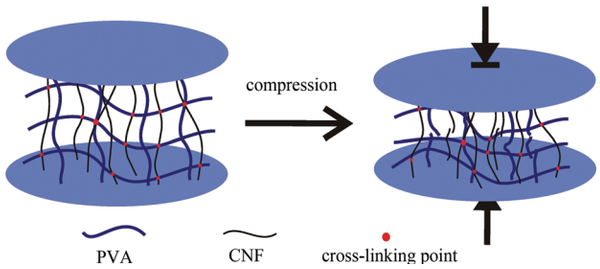

Figure 8. The compression model of composite hydrogels.

4.5. Thermal Stability of Composite Hydrogels

The thermal degradation of PVA and PVA/CNF hydrogels were conducted using TGA as drawn in Figure 9. All samples exhibited three distinct weight loss stages. For the hydrogels without CNF, the first degradation stage at 30–250 °C, can be ascribed to the removal of traces of water vapor (about 8 wt% loss). The second degradation stage between 250 and 380 °C resulted in the highest residual weight loss and this was due to the decomposition of side chain of PVA. And the third decomposition stage at 380–500 °C, can be attributed to the decomposition of main chain of PVA.[15] As shown in Figure 9, major weight losses for the samples without CNF of about 75 wt% were observed in the range of 250–500 °C, which corresponded to the PVA structural decomposition. There was no significant difference in thermal decomposition between pure PVA and 0%CNF/PVA composite hydrogels, indicating hybrid solvent had no effect on the thermal stability of PVA hydrogels during freezing/thawing process.

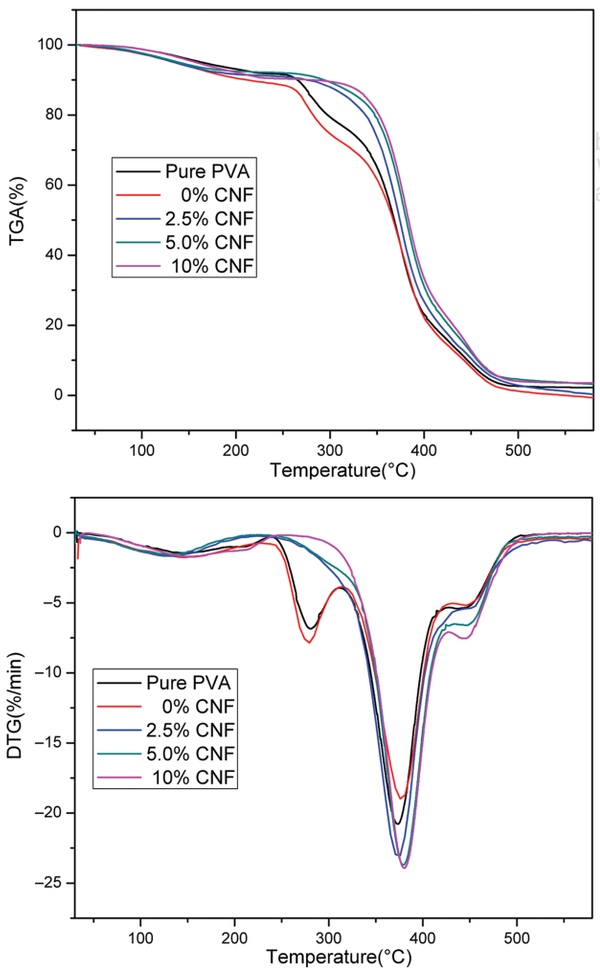

Figure 9. TGA (a) and DTG (b) curves for the composite hydrogels.

As CNF increased, major weight losses were observed in the range of 300–500 °C for all composite hydrogels, which corresponded to the structural decomposition of PVA and thermal degradation of CNF. The onset decomposition temperature corresponding of the CNF/PVA composite hydrogels shifted to a higher temperature compared to that of PVA hydrogels (from 250 to 300 °C). After approximately 500 °C, the curves all became flat, mainly the organic residues were completely volatilized and the inorganic residue remained.[15, 17] And the residues of PVA and 10%CNF/PVA were estimated to be approximately 4 and 9 wt% from the amounts of the residue at 550 °C. Evidently, addition of CNF to PVA hydrogels significantly improved the thermal stability of PVA hydrogels, further proved the presence of the strong hydrogen bonding between CNF and PVA matric.

5. CONCLUSIONS

In conclusion, cellulose nanofibrils (CNF) were obtained from bamboo sawdust by a combination of chemical and mechanical treatments. The results demonstrated that obtained CNF were nanometric size and had adequate thermal stability. Through a combination of hybrid solvent of DMSO/water and freezing/thawing method, porous CNF/PVA hydrogels with controlled structure have been successfully prepared. The average pore size of composites hydrogels shifted from 0.69 μm to 1.09 μm as the content of CNF increased from 2.5 wt% to 10 wt%. Compared with pure PVA hydrogels, the equilibrium swelling ratio of PVA hydrogels prepared from hybrid solvent increased from 568% to 770%. The equilibrium swelling ratio of composites hydrogels increased significantly from 795% to 935% with an increment of CNF content from 2.5 wt% to 10 wt%. A 150% improvement in compressive strength was achieved by the hybrid solvent compared with PVA hydrogels prepared from water alone. Composites hydrogels had the best compressive fracture strength of 0.6 MPa as 2.5 wt% CNF was imparted. The characterization carried out on composites hydrogels demonstrated that the thermal stability was improved significantly with the addition of CNF. In combination with their improved performance, these nanocomposite hydrogels may be suitable for applications in bioengineering and other functional engineering areas.

Acknowledgments: This work was supported by the National Natural Science Foundation of China (Grant No. 31300483), the Natural Science Foundation of Jiangsu Province of China (Grant No. BK20130971) and A Project Funded by the Priority Academic Program Development of Jiangsu Higher Education Institutions (PAPD). We acknowledge Advanced Analysis and Testing Center of Nanjing Forestry University.

References and Notes

1. E. A. Appel, J. del Barrio, X. J. Loh, and O. A. Scherman, *Chem. Soc. Rev.* 41, 6195 (**2012**).
2. B. Balakrishnan and R. Banerjee, *Chem. Rev.* 111, 4453 (**2011**).
3. D. Das, T. Kar, and P. K. Das, *Soft Matter.* 8, 2348 (**2012**).
4. M. A. Karaaslan, M. A. Tshabalala, D. J. Yelle, and G. Buschle-Diller, *Carbohydr. Polym.* 86, 192 (**2011**).
5. H. S. Nalwa (ed.), Encyclopedia of Nanoscience and Nanotechnology, American Scientific Publishers, Los Angeles, CA (**2004**), Vols. 1–10.
6. Y. Wen, R. Harold, Kolonich, N. Giannoukakis, E. S. Gawalt, and W. S. Meng, *Mol. Pharm.* 10, 1035 (**2013**).
7. Y. Wen, W. Liu, B. Christina, S. J. Zhang, M. F. Bai, J. M. Janjica, N. Giannoukakis, E. S. Gawalt, and W. S. Meng, *Acta Biomater.* 10, 4759 (**2014**).
8. K. L. Spiller, S. J. Laurencin, D. Charlton, S. A. Maher, and A. M. Lowman, *Acta Biomater.* 4, 17 (**2008**).
9. M. Lovett, D. Rockwood, A. Baryshyan, and D. L. Kaplan, *Tissue Eng. Part C Methods* 16, 1565 (**2010**).
10. A. Autissier, C. Le Visage, C. Pouzet, F. Chaubet, and D. Letourneur, *Acta Biomater.* 6, 3640 (**2010**).
11. Y. C. Chiu, S. Kocagoz, J. C. Larson, and E. M. Brey, *PloS One* 8, e60728 (**2013**).
12. H. Wu, Y. Wan, X. Cao, and Q. Wu, *Acta Biomater.* 4, 76 (**2008**).
13. S. X. Cheng, J. T. Zhang, and R. X. Zhuo, *Mater. Res.* 67, 96 (**2003**).
14. J. Rouwkema, N. C. Rivron, and C. A. van Blitterswijk, *Trends Biotechnol.* 26, 434 (**2008**).
15. D. Liu, X. Sun, H. Tian, S. Maiti, and Z. Ma, *Cellulose* 20, 2981 (**2013**).
16. S. Taji, M. Nejad-Sadeghi, and I. Goodarznia, *Supercrit Fluids* 95, 603 (**2014**).
17. E. R. Kenawy, E. A. Kamoun, M. S. M. Eldin, and M. A. El-Meligy, *Arab J. of Chem.* 7, 372 (**2014**).
18. H. Jiang, G. Campbell, D. Boughner, W. K. Wan, and M. Quantz, *Med. Eng. Phys.* 26, 269 (**2004**).
19. S. Jiang, S. Liu, and W. Feng, *Biomed Mater.* 4, 1228 (**2011**).
20. P. Calvert, *Adv. Mater.* 21, 743 (**2009**).
21. S. Jiang, Z. Su, X. Wang, S. Liu, and Y. Yu, *Mater Sci. Eng. C* 33, 3768 (**2013**).
22. T. Jiang, G. Wang, J. Qiu, L. Luo, and G. Zhang, *J. Med. Biol. Eng.* 29, 102 (**2009**).
23. W. Chen, H. Yu, and Y. Liu, *Carbohydr. Polym.* 86, 453 (**2011**).
24. Z. Y. Xu, J. Y. Li, H. Zhou. X. D. Jiang, C. Yang, F. Wang, Y. Y. Pan, N. N. Li, X. Y. Li, L. N. Shi, and X. M. Shi, *RSC Adv.* 6, 43626 (**2016**).
25. K. Abe and H. Yano, *Cellulose.* 17, 271 (**2010**).
26. W. S. Rasband, Image J, US National Institutes of Health, Bethesda (MD) (**1997–2014**).
27. H. Tadokoro, S. Seki, and I. Nitta, *J. Polym. Sci.* 22, 563 (**1956**).
28. C. Chang, A. Lue, and L. Zhang, *Chem. Phys.* 209, 1266 (**2008**).
29. K. Chen and Y. Lin, *Enzyme and Microbial Technology* 16, 79 (**1994**).
30. K. Masuda and F. Horii, *Macromolecules* 31, 5810 (**1998**).
31. Y. Hou, C. Chen, K. Liu, Y. Tu, L. Zhang, and Y. Li, *RSC Adv.* 5, 24023 (**2015**).
32. E. A. Kamoun, X. Chen, M. S. M. Eldin, and E. R. S. Kenawy, *Arab J. Chem.* 8, 1 (**2015**).
33. G. Huang, L. Zhou, Q. Zhang, Y. M. Chen, W. Sun, F. Xu, and T. J. Lu, *Biofabrication* 3, 012001 (**2011**).
34. T. Abitbol, T. Johnstone, T. M. Quinn, and D. G. Gray, *Soft Matter.* 7, 2373 (**2011**).
35. F. Yokoyama, I. Masada, and K. Shimamura, *Colloid. Polym. Sci.* 264, 595 (**1986**).
36. A. Autissier, C. Le Visage, C. Pouzet, F. Chaubet, and D. Letourneur, *Acta Biomater.* 6, 3640 (**2010**).
37. L. Z. Ren, P. G. Ren, X. L. Zhang, Z. F. Sun, and Y. Zhang, *Compos. Interfaces* 21, 853 (**2014**).
38. Y. W. Yao, C. Geng, D. Han, F. Chen, and Q. Fu, *RSC Adv.* 4, 39588 (**2014**).

Received: 5 September 2016. Accepted: 15 November 2016.